

Community-Driven Signal Processing On Directed Brain Graphs

Alexandre Cionca^{1,2§}, Chun Hei Michael Chan^{1,2§}, Maria Giulia Preti^{1,2}, Maciej Jedynak³, Yasser Alemán-Gómez⁴,
Olivier David^{3,5}, Patric Hagmann⁴, and Dimitri Van De Ville^{1,2}

¹Neuro-X Institute, École polytechnique fédérale de Lausanne (EPFL), Geneva, Switzerland

²Department of Radiology and Medical Informatics, University of Geneva, Geneva, Switzerland

³Univ. Aix Marseille, Inserm, INS, Institut de Neurosciences des Systèmes, 13005 Marseille, France

⁴ Department of Radiology, Lausanne University Hospital and University of Lausanne (CHUV-UNIL), Lausanne, Switzerland

⁵ Department of Pediatric Neurosurgery, Lenval Foundation Hospital, Nice, France

Abstract—Graphs have become a predominant way of representing structured information. Pioneering frameworks such as graph signal processing (GSP) have been developed for the analysis of data within such representations (e.g. brain graphs). Notably, by integrating community structures, community-aware GSP emphasizes on the importance of capturing the intrinsic organization of the graph, by bringing forth the notion of modularity in the signal analysis. Here, we leverage recent work on community detection for directed graphs and propose a community-driven signal processing approach. Graphs signals are projected through regression onto a dictionary defined by the directed communities, termed bicomunities, to later obtain a decomposition of the original signal. We then apply the proposed framework to brain graphs and signals obtained with magnetic resonance imaging. Our findings provide relevant insights into known functional brain networks and open new avenues for the study of their interaction.

Index Terms—Community structure, modularity, directed graphs, graph signal processing, MRI, brain connectivity

I. INTRODUCTION

Recent years have seen the growth of diverse methods and applications to analyze signals on irregular domains such as graphs. One important example of these efforts is the field of graph signal processing (GSP) [1], [2] that defines operations such as the Graph Fourier Transform (GFT), which then provide the basis for spectral analysis and filtering of graph signals. In literature, the GFT is mostly defined by the eigenvectors of a graph shift operator (GSO), such as the Laplacian or the adjacency matrix [1], [2], [3], [4]. However, another stance can be taken, by considering the modularity matrix as GSO, and therefore integrating the concept of community structure into the operations. Previous work on community-aware GSP [5] has extended the initial GFT with operations such as filtering, sampling, denoising as well as an application to brain graphs. In addition, there is a growing

interest in GSP for directed graphs with several recent works dealing with directed edge information [6], [7], [8].

In this work, we bring the aspects of both community-aware GSP and digraph GSP to propose community-aware signal processing for directed graphs. Specifically, we leverage a newly proposed framework for community detection in directed graphs, entitled *bimodularity* [9], whose foundation lies in separating a community in a sending and its corresponding receiving parts (i.e., a *bicomunity*). We then propose a scheme to decompose a graph signal in terms of those bicomunities. We demonstrate the feasibility of this approach for synthetic data with ground truth, as well as for the directed human connectome. The highlighted communication pathways are put in relationship with brain function by estimating signals that would propagate through the bicomunities to fit known brain functional networks [10]. We finally show that it is possible to split the graph signal according to the sending/receiving properties of the constituting bicomunities.

II. BICOMMUNITY-INFORMED SIGNAL PROCESSING

A. Detection of bicomunities

Let us consider a directed graph \mathcal{G} of cardinality N represented by the asymmetric adjacency matrix \mathbf{A} . From \mathbf{A} we then consider the bimodularity index that is an extension of the well known modularity metric [11], but accounting for graph edges from a sending to its corresponding receiving community [9]:

$$Q_{\text{bi}} = \frac{1}{m} \sum_{k=1}^K \sum_{\substack{i \in C_k^{\text{out}} \\ j \in C_k^{\text{in}}}} [A_{ij} - \mathbf{E}(A_{ij}|\mathcal{H}_0)], \quad (1)$$

where m is the total number of edges, K is the number of bicomunities and $\mathbf{E}(A_{ij}|\mathcal{H}_0)$ expresses the expected proportion of edges under a null hypothesis. The null hypothesis \mathcal{H}_0 expresses homogeneous distribution of edge weights over the nodes; i.e., $k_i^{\text{out}} k_j^{\text{in}} / (2m)$ where k_i^{out} is the out-degree of node i and k_j^{in} is the in-degree of node j [12]. For the case of two bicomunities, Eq. (1) can be rewritten using separator

[§]Equal contribution

This work was supported in part by the Swiss National Science Foundation, Sinergia project “Precision mapping of electrical brain network dynamics with application to epilepsy”, Grant number 209470.

Manuscript received XXX; revised XXX.

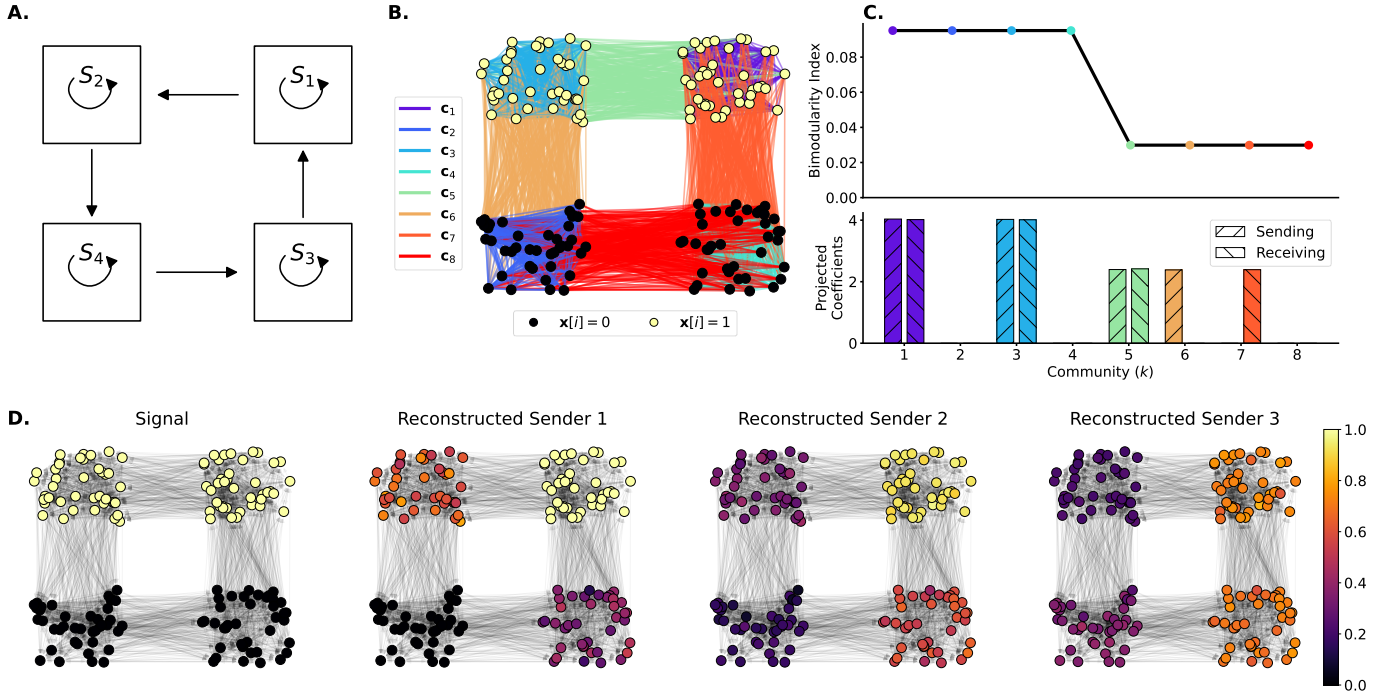


Fig. 1. Canonical example on the block cycle graph. A) Diagram of the directed edges between 4 sets of nodes S_k , $k = 1, \dots, 4$. B) Edge clusters of block cycle graph (see caption) with a graph signal \mathbf{x} located in the upper blocks (S_1, S_2). C) Bimodularity index of each bicomunity (in descending order – top) and projected coefficients \mathbf{w} of the graph signal in B (bottom). D) Reconstructed senders \mathbf{x}^{send} of the graph signal (left) for 1 to 3 repeated steps. Each step takes as input the signal directly on the left ($\mathbf{x}_2^{\text{send}} = \mathbf{C}^{\text{out}} \mathbf{C}^{\text{in}\dagger} \mathbf{x}_1^{\text{send}}$, sender 2 is the reconstructed sender of sender 1).

vectors \mathbf{s}^{out} and \mathbf{s}^{in} , whose elements take values $+1/-1$ to indicate the partitioning

$$Q_{\text{bi}}(\mathbf{s}^{\text{out}}, \mathbf{s}^{\text{in}}) = \frac{1}{m} \sum_{\substack{(i,j) \text{ s.t.} \\ \mathbf{s}^{\text{out}}[i] = \mathbf{s}^{\text{in}}[j]}} B_{ij} = \frac{1}{2m} (\mathbf{s}^{\text{out}})^T \mathbf{B} \mathbf{s}^{\text{in}}, \quad (2)$$

with $B_{ij} = A_{ij} - k_i^{\text{out}} k_j^{\text{in}} / m$ being the directed modularity matrix. Optimization of bimodularity is achieved through convex relaxation that allows \mathbf{s}^{out} and \mathbf{s}^{in} to take real values instead of strictly $+1/-1$ and imposes unitary norms. From (2), the bipartition problem is solved through a spectral approach that maximizes the bimodularity by considering the singular value decomposition (SVD) of the matrix $\mathbf{B} = \mathbf{U} \mathbf{\Sigma} \mathbf{V}^T$. The left \mathbf{U} and right \mathbf{V} singular vectors can therefore be interpreted as describing the space of sending and receiving communities, respectively, and the diagonal elements of $\mathbf{\Sigma}$ are the singular values μ that relate to the bimodularity index, such that $Q_{\text{bi}}(\mathbf{u}_n, \mathbf{v}_n) = \frac{\mu_n}{2m}$.

Beyond the bimodularity embeddings given by \mathbf{U} and \mathbf{V} , the detection of bicomunities is achieved through clustering at the edge level. In particular, a feature space for the graph edges is created by aggregating the sending projection $\mathbf{u}_n[i]$ of the source node i and the receiving projection $\mathbf{v}_n[j]$ of the target node j , both weighted by μ_n , n -th entry of the diagonal matrix $\mathbf{\Sigma}$. Formally, to the edge (i, j) is associated the feature vector:

$$\mathbf{f} = (\mu_1 \mathbf{u}_1[i], \mu_1 \mathbf{v}_1[j], \dots, \mu_N \mathbf{u}_N[i], \mu_N \mathbf{v}_N[j]),$$

The nodal representation of each cluster of edges that will represent a bicomunity, is recovered as the proportion of (out or in) edges which belong to a specific cluster. The sets of sending and receiving nodes for a bicomunity are represented as $\mathbf{c}_k^{\text{out}}$ and \mathbf{c}_k^{in} , respectively.

A consequence of edge clustering is that a node can belong to different bicomunities, similar to link communities for the undirected case [13]. Those sending and receiving sets of nodes can either overlap, thus leading to conventional graph communities of densely connected nodes (assortative), or they can describe directed connections between disjoint sets of nodes in a bipartite-like structure (disassortative) [14].

B. Signal processing on bicomunities

We now propose to consider the graph signal $\mathbf{x} \in \mathbb{R}^N$ and represent it in terms of the graph's sending and receiving communities. Formally, we build the two following matrices

$$\mathbf{C}^{\text{in}} = (\mathbf{c}_1^{\text{in}}, \dots, \mathbf{c}_K^{\text{in}}), \quad \mathbf{C}^{\text{out}} = (\mathbf{c}_1^{\text{out}}, \dots, \mathbf{c}_K^{\text{out}})$$

and regress the weights $\mathbf{w}^{\text{in}}, \mathbf{w}^{\text{out}}$ so that

$$\mathbf{w}^{\text{in}} = \underset{\mathbf{w} \in \mathbb{R}^K}{\text{argmin}} \|\mathbf{x} - \mathbf{C}^{\text{in}} \mathbf{w}\|^2, \quad \mathbf{w}^{\text{out}} = \underset{\mathbf{w} \in \mathbb{R}^K}{\text{argmin}} \|\mathbf{x} - \mathbf{C}^{\text{out}} \mathbf{w}\|^2.$$

To do so, let $\mathbf{C}^{\text{in}\dagger}, \mathbf{C}^{\text{out}\dagger}$ be the pseudo-inverse of the above-mentioned matrices, then the weights for optimal signal representations are given by:

$$\mathbf{w}^{\text{in}} = \mathbf{C}^{\text{in}\dagger} \mathbf{x}, \quad \mathbf{w}^{\text{out}} = \mathbf{C}^{\text{out}\dagger} \mathbf{x}.$$

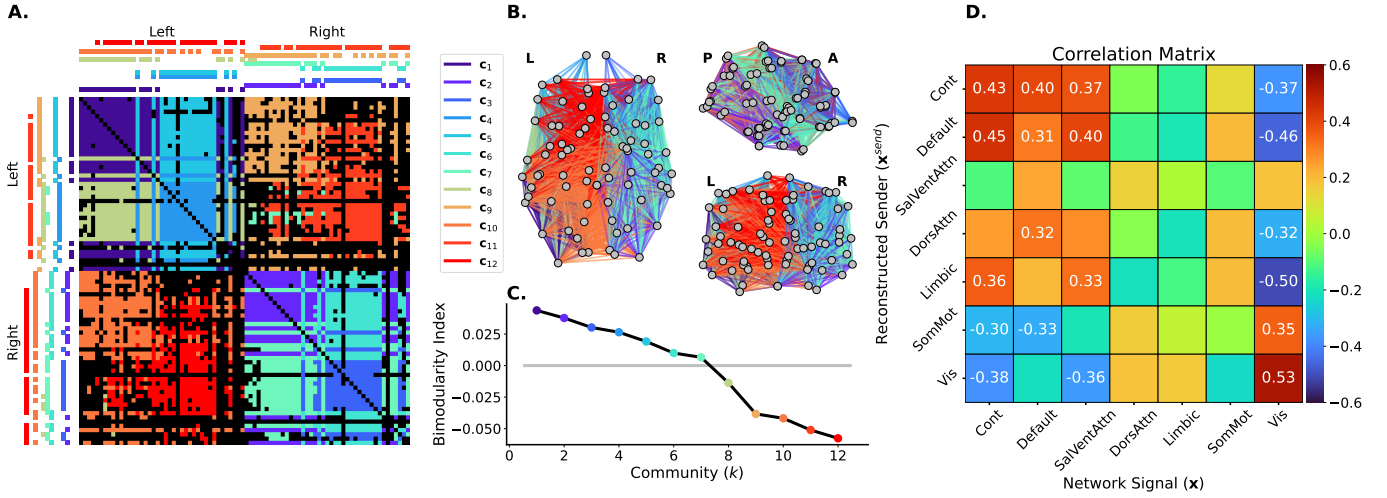


Fig. 2. Brain bicomunities and signal sender reconstruction. A) 12 brain communities $c_1 - c_{12}$ are shown in different colors (see caption), including block diagonals representing *assortative communities*, off-diagonal blocks in upper left and lower right squares showing *within-hemisphere communities*, and upper right and lower left squares showing *between-hemisphere communities*. B) Brain views of the communities. L: left; R: right; A: anterior; P: posterior. C) Bimodularity index of communities, shown in decreasing order. D) Pearson correlation between the reconstructed sender \mathbf{x}^{send} of each resting-state network and the network themselves (values are shown for $|\rho| \geq 0.3$). A high positive value in row i and column j denotes that the nodal representation of network j could originate from network i . Brain networks abbreviations are Cont: Control; SalVentAttn: Salience Ventral Attention; DorsAttn: Dorsal Attention; SomMot: Somatosensory Motor; Vis: Visual.

Therefore, $\tilde{\mathbf{x}}^{\text{in}} = \mathbf{C}^{\text{in}} \mathbf{w}^{\text{in}}$ and $\tilde{\mathbf{x}}^{\text{out}} = \mathbf{C}^{\text{out}} \mathbf{w}^{\text{out}}$ represent the fitted signals in terms of a linear combination of the receiving and sending communities, respectively.

One avenue to aggregate sending and receiving information is to leverage the correspondence between a receiving community and its sending pattern. While \mathbf{w}^{in} captures the optimal weights to reconstruct \mathbf{x} using the receiving communities \mathbf{C}^{in} , these weights can also be used for reconstruction with the sending communities \mathbf{C}^{out} . Intuitively, $\mathbf{x}^{\text{send}} = \mathbf{C}^{\text{out}} \mathbf{w}^{\text{in}}$ computes the signal that would lead to \mathbf{x} through the bicomunities: the reconstructed sender. Similarly, the propagation of the signal through the bicomunities, or the reconstructed receiver, can be estimated as $\mathbf{x}^{\text{receive}} = \mathbf{C}^{\text{in}} \mathbf{w}^{\text{out}}$.

III. RESULTS

A. Synthetic data

As a first proof of concept, we consider the directed block cycle graph with four sets of nodes that have connections within themselves and between them according to the directional pattern indicated in Fig. 1.A. Eight bicomunities are retrieved, Fig. 1.B, and can be distinguished as assortative or dissortative based on their bimodularity index in Fig. 1.C.

A synthetic binary graph signal is considered, with non-zero values in the two upper blocks (1.B). We first observe that the weights associated to each communities in 1.C are higher for assortative (purple and blue) than dissortative communities. This is consistent with the fact that this block cycle graph is more densely connected within blocks than between blocks.

We then compute the reconstructed sender $\mathbf{x}^{\text{send}} = \mathbf{C}^{\text{out}} \mathbf{C}^{\text{in}^\dagger} \mathbf{x}$ for a synthetic graph signal in two consecutive blocks (Fig. 1.D). The first reconstructed sender signal (sender 1) is concentrated in the upper right block with less energy

in the other upper block (S_2) and even less in the lower right block (S_3). Further reconstruction of the senders (considering the previous sender as graph signal) shows a smooth transition from signal concentration in the upper blocks (original signal) to signal concentration in the blocks on the right (sender 3). Because the columns of \mathbf{C} and rows of \mathbf{C}^\dagger do not form a complete basis, the signal reconstruction is not perfect, and this is translated in a decrease in the signal norm and contrast.

B. Human brain

A directed human connectome is built by aggregating a population-level white-matter bundle atlas [15] and cortico-cortical evoked potentials (CCEP) from stereo-encephalographic responses to direct electrical stimulation of the multi-centric F-TRACT database [16]. Specifically, the probability to have a bundle is used to compute the strength of connections s_{ij} between two brain regions i and j . The directionality of connections is estimated from the directed communication f_{ij} which represents the probability to record an early CCEP ($< 100\text{ms}$) in area j when stimulating area i . The directed connectivity d_{ij} is then derived by redistributing the connectivity strength to the outgoing or incoming connection based on the proportion of outgoing or incoming communication probability:

$$d_{ij} = 2s_{ij} \frac{f_{ij}}{f_{ij} + f_{ji}}.$$

We first extract $K = 12$ bicomunities (based on silhouette analysis) from this directed brain connectome (Fig. 2.A). These cluster of edges (Fig. 2.B) capture, in descending order of bimodularity index (Fig. 2.C): assortative communities within the anterior or posterior half of each hemisphere (c_1

to c_4); anteroposterior communication within each hemisphere (c_5 to c_8); and inter-hemispheric connections (c_9 to c_{12}).

Similar to the canonical block cycle example, we compute the reconstructed sender of known functional brain networks [10]. Nodal signals reflect the probability that a given node belongs to a particular brain network. Fig. 2.D shows the Pearson correlation of each pair of reconstructed sender (row) and original network (column). As such, we observe high correlation between the nodal representation of higher-level networks (control, default, salience) and their reconstructed senders. On the other hand, the visual network appears to originate from itself or from the somatosensory motor network. The senders reconstructed with $K = 12$ do not overlap with the dorsal attention, limbic and somatosensory motor networks.

IV. DISCUSSIONS & OUTLOOK

We took advantage of the recently introduced notion of bicomunities, which are communities endowed with directionality. We introduce the idea of bicomunity-driven coefficients of a graph signal and discuss how these coefficients can be used to reconstruct a signal that has been propagated through the bicomunities.

This is unique to directed graphs and, especially, to the correspondence between the sending and receiving parts of a bicomunity, introduced in [9]. Relevant investigation could incorporate sender/receiver reconstruction with a selected subset of bicomunities or after operating on the projected coefficients w . Extra attention is needed because perfect reconstruction is, in general, not feasible since the columns of C do not form a basis. Partial reconstruction using a subset of bicomunities nevertheless remains a compelling avenue.

The bicomunities of the directed human connectome capture the hemispheric and anteroposterior axes of brain communication. High-level networks of the brain tend to emerge from one another, aligning with the notion that they are broadly distributed and that higher-level functions are dynamically reorganizing. On the other hand, primary sensory networks, such as visual and somatomotor, appear more segregated. This aligns well with literature that identified a macroscale gradient opposing low-level sensory to high-level cognition networks based on different perspectives (e.g., temporal hierarchy, coupling between structure and function) [17], [18], [19]. Consistent with our results, work on global workspace applied to the brain also identified high-level regions (default mode and attention area) as part of a rich club orchestrating information throughout the brain [18]. These are specific to the identified bicomunities, but lower level processes (sensory) could however be observed with more bicomunities.

Our work adds to the existent studies bringing a new perspective on directed graph signal processing, that holds significant relevance for applications such as in network neuroscience.

CODE AND DATA

All code and data used in this article are openly available at <https://github.com/MIPLabCH/Bimodularity>.

ACKNOWLEDGMENT

This work was supported in part by the Swiss National Science Foundation in the context of the Sinergia ‘‘Precision mapping of electrical brain network dynamics with application to epilepsy’’, grant number 209470.

REFERENCES

- [1] D. I. Shuman, S. K. Narang, P. Frossard, A. Ortega, *et al.*, ‘‘The emerging field of signal processing on graphs: Extending high-dimensional data analysis to networks and other irregular domains,’’ *IEEE Signal Processing Magazine*, vol. 30, pp. 83–98, May 2013.
- [2] A. Ortega, P. Frossard, J. Kovacević, J. M. F. Moura, *et al.*, ‘‘Graph Signal Processing: Overview, Challenges, and Applications,’’ *Proceedings of the IEEE*, vol. 106, pp. 808–828, May 2018.
- [3] A. Sandryhaila and J. M. F. Moura, ‘‘Discrete Signal Processing on Graphs,’’ *IEEE Transactions on Signal Processing*, vol. 61, pp. 1644–1656, Apr. 2013.
- [4] W. Huang, T. A. W. Bolton, J. D. Medaglia, D. S. Bassett, *et al.*, ‘‘A Graph Signal Processing Perspective on Functional Brain Imaging,’’ *Proceedings of the IEEE*, vol. 106, pp. 868–885, May 2018.
- [5] M. Petrovic, R. Liegeois, T. A. Bolton, and D. Van De Ville, ‘‘Community-Aware Graph Signal Processing: Modularity Defines New Ways of Processing Graph Signals,’’ *IEEE Signal Processing Magazine*, vol. 37, pp. 150–159, Nov. 2020.
- [6] R. Shafipour, A. Khodabakhsh, G. Mateos, and E. Nikolova, ‘‘A Directed Graph Fourier Transform With Spread Frequency Components,’’ *IEEE Transactions on Signal Processing*, vol. 67, pp. 946–960, Feb. 2019.
- [7] S. Kwak, L. Shimabukuro, and A. Ortega, ‘‘Frequency Analysis and Filter Design for Directed Graphs with Polar Decomposition,’’ in *ICASSP 2024 - 2024 IEEE International Conference on Acoustics, Speech and Signal Processing (ICASSP)*, (Seoul, Korea, Republic of), pp. 9661–9665, IEEE, Apr. 2024.
- [8] C. H. M. Chan, A. Cionca, and D. Van De Ville, ‘‘Hilbert Transform on Graphs: Let There Be Phase,’’ *IEEE Signal Processing Letters*, vol. 32, pp. 1725–1729, 2025.
- [9] A. Cionca, C. H. M. Chan, and D. V. D. Ville, ‘‘Community detection for directed networks revisited using bimodularity,’’ Feb. 2025. arXiv:2502.04777 [cs].
- [10] B. T. Thomas Yeo, F. M. Krienen, J. Sepulcre, M. R. Sabuncu, *et al.*, ‘‘The organization of the human cerebral cortex estimated by intrinsic functional connectivity,’’ *Journal of Neurophysiology*, vol. 106, pp. 1125–1165, Sept. 2011. Publisher: American Physiological Society.
- [11] M. E. J. Newman, ‘‘Modularity and community structure in networks,’’ *Proceedings of the National Academy of Sciences*, vol. 103, pp. 8577–8582, June 2006. Publisher: Proceedings of the National Academy of Sciences.
- [12] E. A. Leicht and M. E. J. Newman, ‘‘Community Structure in Directed Networks,’’ *Physical Review Letters*, vol. 100, p. 118703, Mar. 2008.
- [13] Y.-Y. Ahn, J. P. Bagrow, and S. Lehmann, ‘‘Link communities reveal multiscale complexity in networks,’’ *nature*, vol. 466, no. 7307, pp. 761–764, 2010.
- [14] T. A. Snijders and K. Nowicki, ‘‘Estimation and Prediction for Stochastic Blockmodels for Graphs with Latent Block Structure,’’ *Journal of Classification*, vol. 14, pp. 75–100, Jan. 1997.
- [15] Y. Alemán-Gómez, A. Griffa, J.-C. Houde, E. Najdenovska, *et al.*, ‘‘A multi-scale probabilistic atlas of the human connectome,’’ *Scientific Data*, vol. 9, p. 516, Aug. 2022.
- [16] J.-D. Lemaréchal, M. Jedynak, L. Trebaul, A. Boyer, *et al.*, ‘‘A brain atlas of axonal and synaptic delays based on modelling of cortico-cortical evoked potentials,’’ *Brain*, vol. 145, pp. 1653–1667, May 2022.
- [17] M. G. Preti and D. Van De Ville, ‘‘Decoupling of brain function from structure reveals regional behavioral specialization in humans,’’ *Nature Communications*, vol. 10, p. 4747, Oct. 2019. Publisher: Nature Publishing Group.
- [18] G. Deco, D. Vidaurre, and M. L. Kringelbach, ‘‘Revisiting the global workspace orchestrating the hierarchical organization of the human brain,’’ *Nature Human Behaviour*, vol. 5, pp. 497–511, Apr. 2021. Publisher: Nature Publishing Group.
- [19] C. Baldassano, J. Chen, A. Zadbood, J. W. Pillow, *et al.*, ‘‘Discovering event structure in continuous narrative perception and memory,’’ *Neuron*, vol. 95, no. 3, pp. 709–721, 2017.